energy&fuels

Article

pubs.acs.org/EF

Uncertainty Analysis of the Mercury Oxidation over a Standard SCR Catalyst through a Lab-Scale Kinetic Study

Ana Suarez Negreira* and Jennifer Wilcox

Department of Chemical Engineering, and Department of Energy Resources Engineering, Stanford University, 450 Serra Mall, Stanford, California 94305, United States

Supporting Information

ABSTRACT: A kinetic study of the mercury oxidation across a standard composition SCR catalyst under simplified flue gas conditions (12 % CO_2, 5 % O_2, 5 % H_2O, 5 ppb Hg, 10 ppm of HCl in air) is carried out in a lab-scale packed-bed reactor. A thorough analysis is presented of the experimental error on the Hg oxidation rates, reaction orders, and activation energy propagated from the uncertainty in the measured mercury concentrations, thereby revealing several important limitations of these lab-scale experiments. The effects are investigated of flue gas composition, temperature, and space velocity on the Hg oxidation efficiency of the catalyst, and the reaction order of O_2 and Hg are derived together with the apparent activation energy. It is confirmed that O_2 is zeroth-order while Hg is first-order in terms of the Hg oxidation rate. An activation energy of 34 ± 7 kJ/mol is obtained. It is shown that the magnitude of the oxidation efficiencies increases with increasing amount of catalyst and temperature (from 150 to 350 °C).

INTRODUCTION

Mercury emissions from the power sector accounted for 28 % of the total anthropogenic mercury emissions (approximately 1600 tons) in 2010, but it is projected to represent 50 % of the global emissions by 2050 (estimated to be ≈2660 tons). While current models suggest a stabilization or decline in the Hg emissions from Europe and United States, mercury releases from the fast growing economies of China and India will increase.[1] These emissions have a global impact due to the long lifetime (6 to 12 months) of elemental mercury (Hg^0) in the atmosphere together with the long distances that it can travel, thus putting millions of people at risk.[2]

This increasing public concern due to the long-term irreversible effects of mercury on the environment and human health (neurocognitive deficits in children and impaired cardiovascular health in adults) has driven stricter regulations of the Hg emissions.[3,4] In October of 2013, more than 140 nations signed a legally binding treaty on reductions in human uses and releases of mercury.[2] This followed the effort of the U.S. Environmental Protection Agency (EPA) that in 2011 proposed the Mercury and Air Toxics Standards (MATS), which required U.S. natural gas and coal-fired power plants to install air pollution control devices to prevent 91 % of the Hg present in flue gas from being released.[5]

Currently, there are several air pollution control devices designed to reduce Hg emissions in power plants and whose working principles depend on the nature of the mercury species. Mercury is present in the flue gas in three forms: elemental (Hg^0), oxidized (Hg^{2+}), and particulate-bond (Hg^P).[6] Oxidized Hg is highly soluble in aqueous solutions, as compared to the insoluble and nonreactive Hg^0, thus allowing for the removal of the former by conventional air pollution control devices.[7−9]

Under typical postcombustion conditions (i.e., 1 atm and 700 °C), the homogeneous oxidation of mercury is kinetically limited,[10] and it is responsible for only 10 % of the total mercury oxidation.[11,12] The extent of the gas-phase oxidation reaction is also controlled by the presence of oxidizing species such as Cl_2, HCl, chlorine radicals, and ozone.[13] The heterogeneous oxidation of mercury is the dominant oxidation mechanism under postcombustion conditions.[13] The catalytic oxidation of mercury can be obtained as a cobenefit of existing control technologies such as the Selective Catalyst Reduction (SCR) unit for NOx reduction [14] This option is particularly attractive due to the associated low economic investment, since 40 % of electricity from coal sources is produced in power plants that are already equipped with SCR units.[15]

The oxidation of mercury across the SCR catalyst has been extensively studied across different scales, from bench[16,17]-to-power-plant scale,[9,18−20] confirming negligible Hg oxidation activity on the SCR catalyst when HCl is absent. The presence of HCl in the flue gas, which is coal-type dependent,[21,22] has a dramatic effect on the Hg^0 oxidation activity.[23−25] The combustion of bituminous coal, which generally contains a high HCl concentration, results on oxidation efficiencies of 90 % across the SCR units, whereas much lower oxidation efficiencies (less than 30 %) were measured in power plants burning sub-bituminous coal, whose HCl concentration is less than 100 ppm.[22,23] Both experimental[16,17] and theoretical studies[26,27] report higher affinity of HCl for the active sites as compared to Hg on vanadia−titania and vanadia−tungsten−titania based SCR catalysts.

To date most of the experimental studies were performed with the aim of determining Hg oxidation efficiencies with little kinetic analysis done across the SCR catalysts.[28] A kinetic analysis can provide important information, such as oxidation

Received: September 17, 2014
Revised: November 3, 2014
Published: November 4, 2014

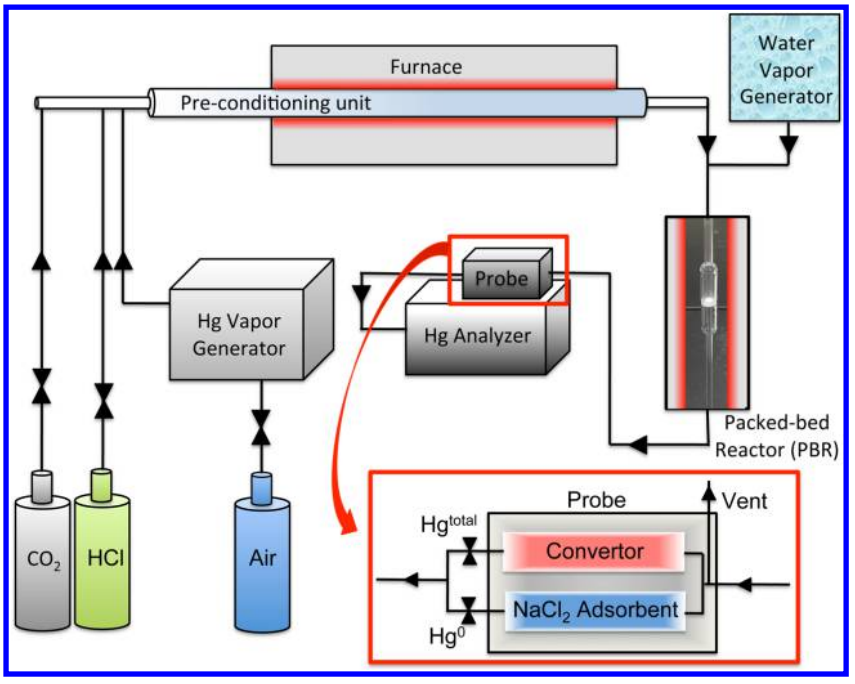

Figure 1. Lab set-up for Hg oxidation experiments. The inset corresponds to a schematic representation of the pre-conditioning probe of the Hg analyzer. The convertor unit transforms Hg^{2+} to Hg^0 when Hg^{tot} is measured, while the NaCl adsorbent unit captures Hg^{2+} when Hg^0 is measured.

rates, reaction orders, and activation energies, which are key to select potential commercial catalysts based on lab-scale results. Even scarcer are the studies reporting the *uncertainty* associated with the measurements of mercury concentrations and the propagated error on any parameter that depends on these concentrations. To our knowledge, none of the studies on Hg oxidation across SCR catalysts includes an error analysis and the reliability of the reported data may therefore be questioned.

The effects are revisited of flue gas composition, temperature, and space velocity on the mechanism driving mercury oxidation across a standard SCR catalyst under these flue gas conditions: 12 % CO_2, 5 % O_2, 5 % H_2O, 5 ppb Hg, 10 ppm of HCl in air. The analysis of the oxidation of Hg covered in this study does not include the presence of the DeNOx reaction, where NO_x is reduced to inert N_2 through the interaction with NH_3 and the SCR catalyst sites. It is well-known that the DeNOx reaction has a strong influence on mercury oxidation since both reactions compete for active sites of the SCR catalyst[21,29,30] and, under some operating conditions, oxidized mercury can be reduced by NH_3.[24,31] While we acknowledge the importance of including NH_3 in the simulated flue gas to get a more accurate representation of a real SCR operating conditions, NH_3 could not be used in this study because of limitations in the lab set-up, which are explained in the section on experimental condition. Therefore, although the conditions tested in this work may be limited to truly represent the operating conditions of a commercial SCR catalyst, the novelty comes in discussing the accuracy of those measurements. It is not the purpose of this work to report reaction rates or kinetic parameters for Hg oxidation under such a complex flue gas composition but rather to carry out a thorough analysis of the experimental error on these parameters propagated from the uncertainty on the measured mercury concentrations under simplified (but well controlled) combustion conditions. Little benefit could be obtained by adding complexity to the oxidation reaction if the uncertainty of measuring Hg concentrations, oxidation rates, and kinetic parameters under simple combustion conditions are not yet understood and quantified.

This work aims at showing that reliability in any Hg analysis should be assessed through the ability in measuring Hg concentration in a reproducible manner. Deviations from these ideal conditions should quantified in the error analysis that is the key to further quantify the uncertainty in any variable estimated from these measurements. The results of our work represents a first step toward a more comprehensive kinetic study on Hg oxidation across the SCR catalyst. Research groups capable of performing tests at more realistic SCR operating conditions can benefit from our study since this uncertainty analysis can be easily extended to other experimental conditions.

EXPERIMENTAL MEASUREMENTS

Materials. The SCR catalyst used in this work is a standard vanadia−tungsten−titania catalyst (1 % wt. $VO_{2.5}$-10 % wt. WO_3−TiO_2) which is the typical formulation used at industrial scale. Due to size constraints of the laboratory set-up, the catalysts tested are powdered samples with a particle size distribution of 300−350 μm. The catalyst samples were pelletized and ground to obtain this specific and uniform particle size. Fresh catalyst was used in each new experiment so the "seasoning" effect was not included on the performance of the catalysts, and neither was included the effect of the catalyst configuration (honeycomb vs plate). The catalyst samples were pre-conditioned (heated to testing temperature and exposed to air) for 5 h prior to the experiments. All samples tested were provided by Johnson Matthey Technology Center (Reading, U.K.).

Apparatus. The laboratory set-up simulates postcombustion flue gas conditions by mixing and heating gases in stoichiometric ratios to reach a given flue gas composition. A schematic diagram of the lab set-up is shown in Figure 1 and a full description of the equipment is presented in the Supporting Information. Briefly, the system consists of the pre-conditioning unit, the Hg generator (Cavkit, PSA 10.536 Mercury Calibration System, PS Analytical, U.K.), the packed-bed reactor (SCR reactor, 28 in-long quartz tube with a inner diameter of 0.5 in. surrounded by a 20 in-long ceramic fiber heater), pre-conditioner probe (PSA S123P200 Dilution Probe with Speciation, PS

dx.doi.org/10.1021/ef502096r | Energy Fuels 2015, 29, 369−376

Table 1. List of Experiments and the Compositions of Simulated Flue Gas

experiment	catalyst weight (mg)	gas composition	temp. (°C)
baseline	50	12 % CO_2, 5 % O_2, 5 % H_2O, N_2, 5 ppb Hg	250−350
Test 1:	50	12 % CO_2, 5 % O_2, 5 % H_2O, N_2, 5 ppb Hg, 10 ppm of HCl	150−250−350
effect of C_{O_2}	50	12 % CO_2, 7.5 % O_2, 5 % H_2O, N_2, 5 ppb Hg, 10 ppm of HCl	150−250−350
	50	12 % CO_2, 10 % O_2, 5 % H_2O, N_2, 5 ppb Hg, 10 ppm of HCl	150−250−350
Test 2:	50	12 % CO_2, 5 % O_2, 5 % H_2O, N_2, 5 ppb Hg, 10 ppm of HCl	250−300−350
effect of C_{Hg}	50	12 % CO_2, 5 % O_2, 5 % H_2O, N_2, 10 ppb Hg, 10 ppm of HCl	250−300−350
	50	12 % CO_2, 5 % O_2, 5 % H_2O, N_2, 15 ppb Hg, 10 ppm of HCl	250−300−350
Test 3:	75, 150, 225	12 % CO_2, 5 % O_2, 5 % H_2O, N_2, 15 ppb Hg, 10 ppm of HCl	250−300−350
space velocity	75, 150, 225	12 % CO_2, 5 % O_2, 5 % H_2O, N_2, 15 ppb Hg, 10 ppm of HCl	250−300−350
	75, 150, 225	12 % CO_2, 5 % O_2, 5 % H_2O, N_2, 15 ppb Hg, 10 ppm of HCl	250−300−350

Analytical, U.K.) and online continuous commercial Hg analyzer (Ohio Lummex, RA-915+ model). To reduce the interaction and adsorption of mercury with parts of the system all glassware is made of quartz, Teflon transport lines are used, and the Teflon lines and other components of the lab set-up were heated above the condensation temperature of Hg.

As shown in Figure 1, CO_2, air, HCl, and Hg are fed, mixed and heated to 1000 °C in the pre-conditioning unit (40 in-long quartz tube with a inner diameter of 2 in.). Prior to entering the packed-bed reactor, water vapor is introduced in stoichiometric ratios to complete the flue gas composition leaving the pre-conditioning unit. The packed-bed reactor is connected to the Hg analyzer pre-conditioner probe, as shown in the inset of Figure 1. The Hg^{tot} consists of the mercury that did not get oxidized, Hg^0, and the oxidized mercury, Hg^{2+}; the latter requires reduction in the probe before reaching the analyzer, since the Hg analyzer can only detect Hg^0. The concentration of oxidized mercury, Hg^{2+}, is measured as the difference between the concentrations Hg^{tot} and Hg^0 exiting the reactor. Since Hg^0 is less reactive than Hg^{2+}, it is reasonable to assume that it does not interact as much with the walls of the systems as the oxidized form does. For this reason, the extent of oxidation may be monitored through the change in the concentrations of Hg^0 as

$$X_{Hg} = \frac{C^{in}_{Hg^0} - C^{out}_{Hg^0}}{C^{in}_{Hg^0}} \quad (1)$$

Experimental Conditions. Heterogeneous Hg oxidation across the SCR catalyst was studied under various simulated flue gas conditions with a total gas flow rate, Q, of 1300 mL/min. All tested flue gases contain an extremely low concentration of HCl (10 ppm), which can be associated with a sub-bituminous coal. This concentration of HCl ensures low mercury oxidation efficiencies that are required in the kinetic analysis.

Table 1 summarizes the experiments carried out to confirm with previous studies the role of O_2 and Hg concentrations, temperature and space velocity on the mercury oxidation efficiency. To test the influence of each factor, all of the other parameters were kept constant.

To ensure that the inlet mercury concentration remained constant during the experiment, the inlet flow of mercury was measured before and after each experiment using an empty reactor, and reasonable similar concentrations were recorded. Furthermore, it was observed a small but constant decrease in the Hg signal over time, which is due to a drift in the measurement itself (Hg analyzer) rather than a change in the Hg inlet concentration. This drift has been consistently observed during various tests with an empty reactor that lasted over a period of 12 h. The Hg signal (unit of signal/second) was corrected by assuming a linear decrease in the signal over time by using the initial and final Hg reading obtained from a calibration before and after the experiment.

The baseline experiment was carried out to confirm that the Hg mass balance was satisfied ($C^{in}_{Hg^0} = C^{out}_{Hg^0}$). Test 1 and Test 2 were performed at three different temperatures to establish the reaction order of O_2 and Hg on the Hg oxidation rate, respectively.

Test 3 was performed to understand the effect of space velocity on the Hg efficiency and to obtain reaction constants and an activation energy value. The space velocity, which relates the amount of catalyst with the total flow fed into the system, is defined as

$$SV = \frac{Q}{V} = \frac{Q}{\frac{W}{\rho}} \quad (2)$$

where Q is the total flow rate (L/min), ρ is the density of the catalyst (g/L) and W is the amount of catalyst (g). To vary the space velocity, we chose for simplicity to change the amount of catalyst, instead of changing the total flow rate, Q. The space velocities tested, which are summarized in Table 2, are larger than those at actual SCR operations

Table 2. Effect of the Space Velocity and Temperature on the Hg Oxidation Efficiency (in %)

W (g)	SV (h^{-1})	X at 200 °C	X at 250 °C	X at 300 °C	X at 350 °C
0.075	1 040 000	10	47	54	63
0.150	52 000	30	67	88	94
0.225	34 666	40	71	98	95

(4000−8000 h^{-1}) but in the same range as another laboratory study that used powdered SCR catalysts samples. The work by Chen et al.[32] evaluates the performance of powdered SCR catalyst testing spaces velocities between 50 000 and 150 000 h^{-1}. The catalysis configuration (powdered samples vs honeycomb) is the responsible of the difference in the space velocities between laboratory and real SCR conditions.

The analysis of the oxidation of Hg covered in this study does not include the presence of the DeNOx reaction, where NO_x is reduced to inert N_2 through the interaction with NH_3 and the SCR catalyst sites. NH_3 could not be used in this study because of limitations in the lab set-up. In particular, it was observed that when 400 ppm of NH_3 were added in the simulated flue gas, NH_3 reacted with HCl and water vapor forming a complex salt that coated some of the optical components of the Hg analyzer (the components not heated within the analyzer). As a result of this deposition, the capacity of the Hg analyzer to read accurate concentrations was compromised.

METHODS

Kinetic Analysis of Packed-Bed Reactors. The concepts explained in this section are extensively described in Fogler[33] and summarized in the Supporting Information. With respect to the latter, only the final equations are shown here. For a packed-bed reactor at steady-state, the reaction rate expressed as a function of the differential mass of catalyst is

$$r_{Hg} = F^{in}_{Hg}\frac{dX}{dW} \approx F^{in}_{Hg}\frac{X}{W} \quad (3)$$

where W is the mass of the solid catalyst, F^{in}_{Hg} is the molar feed rate of Hg at the inlet (mol/min), and X is the oxidation efficiency, which relates the inlet and outlet molar feed rate of Hg as $F_{Hg} = F^{in}_{Hg}(1 - X)$.

dx.doi.org/10.1021/ef502096r | Energy Fuels 2015, 29, 369−376

The assumption of a linear relationship between X and W is supported in the Results section of this work.

On the other hand, the rate of disappearance of Hg is carried out around the limiting reactant, (i.e., Hg) and it is dependent on the temperature and the concentrations of the gas species as

$$r_{Hg} = -k_{Hg} C_{Hg}^{a} C_{O_2}^{b} C_{HCl}^{c} \quad (4)$$

where a, b, and c are the reaction order of O_2, Hg, and HCl, respectively and $-k_{Hg}$ is the rate constant.

Kinetic Analysis: Mechanism and Rate-Limiting Steps. To explain the heterogeneous oxidation of Hg across the SCR catalyst, an Eley−Rideal mechanism is assumed where HCl adsorbs on the surface to later react with Hg in the gas phase. This mechanism is chosen due to the weak interaction of Hg with the SCR catalyst under flue gas conditions, reported previously both experimentally[16,17] and theoretically.[26,27] Although other gas components such as O_2 could play a role on the Hg oxidation through the formation of HgO species, it will be shown in the Results section that the Hg oxidation mechanism is zeroth-order with respect to O_2 (and first order with respect to Hg). For this reason, the concentration of O_2 is not included in any of the steps of the proposed mechanism described in the following, where S is a surface site:

1. Adsorption $HCl_{(g)} + S \leftrightarrow HCl{\cdot}S$
2. Surface reaction $Hg_{(g)} + HCl{\cdot}S \leftrightarrow HgHCl{\cdot}S$
3. Desorption $HgHCl{\cdot}S \leftrightarrow HgCl_{(g)} + H{\cdot}S$

For each of these steps, it is possible to write an expression for the forward and backward reactions and their full description can be found in the Supporting Information. Due to the smaller concentration of Hg compared to HCl in the gas phase ($C_{Hg}^{(g)}$ is in ppb levels while $C_{HCl}^{(g)}$ in ppm levels), it can be assumed that the surface reaction between adsorbed HCl and gas-phase Hg is the rate-limiting step, which expression is

$$r_{SR} = -k_F C_{Hg} C_S \theta_{HCl} + k_B C_{HgCl} C_{H\cdot S} = -k_F \left[C_{Hg} C_S \frac{K_{ADS} C_{HCl}}{1 + K_{ADS} C_{HCl}} + \frac{C_{HgCl} C_{H\cdot S}}{K_{DES} K_{SR}} \right] \quad (5)$$

where k_F and k_B are the forward and backward rate constants of the surface reaction, respectively. The species concentrations on the surface, C_{HgCl}, $C_{H\cdot S}$, and θ_{HCl} are rewritten in terms of the adsorption and desorption reaction expressions. On the right side of eq 5, K_{ADS} ($K_{ADS} = k_{A-}/k_A$) is equilibrium constant for the adsorption step, K_{SR} ($K_{SR} = k_B/k_F$) is the equilibrium constant for the surface reaction step, and K_{DES} ($K_{DES} = k_{D-}/k_D$) is the equilibrium constant for the desorption step, respectively.

The second term inside the bracket in eq 5 can be considered negligible compared to the first term, since the concentrations of HgCl and surface-adsorbed H are much smaller than concentration of HCl and surface sites (C_{HCl} and C_S), therefore, $C_{HgCl\cdot}C_{H\cdot S} \approx 0$. Furthermore, due to the larger concentration of surface sites and HCl compared to the concentration of Hg^0, it is possible to assume that these concentrations are not changing during the reaction and they can be included in an effective rate constant, k_{eff} as

$$r_{SR} = -k_F \left[C_{Hg^0}^{in} (1 - X) C_S \frac{K_{ADS} C_{HCl}}{1 + K_{ADS} C_{HCl}} \right] = k_{eff} C_{Hg^0}^{in} (1 - X) \quad (6)$$

Finally, combining eq 3 and eq 6 and integrating, the resulting expression relates the change in the oxidation efficiency with the amount of catalyst, W (if the total volumetric flow, Q, is kept constant) as

$$k_{eff} C_{Hg^0}^{in} (1 - X) = F_{Hg}^{in} \frac{dX}{dW} \rightarrow -\ln(1 - X) = k_{eff} \frac{W}{Q} \quad (7)$$

By changing the amount of catalyst, W, with temperature for a given catalyst and flue gas composition, it is possible to obtain the k_{eff} from the slopes, when $-\ln(1 - X)$ is plotted as a function of W. The different reaction rate constants, k_{eff}, obtained at different temperatures can be fitted in the Arrhenius equation to obtain the apparent activation energy, E_A, from the following equation:

$$k_{eff} = k_0 \, e^{-E_A/RT} \rightarrow -\ln(k_{eff}) = -\ln(k_0) - \frac{E_A}{RT} \quad (8)$$

where k_0 is the pre-exponential factor, E_A is the apparent activation energy (J/mol), R is the gas constant (8.314 J/mol·K), and T is the absolute temperature (K).

Assessment of the Hg Measurements Precision. One of the limitations in the evaluation of the Hg oxidation efficiency is the difficulty in measuring such small Hg concentrations in an accurate and reproducible way. The low concentrations of mercury in the flue gas (low ppb levels) require long exposure times of the catalyst to the flue gas for the system to reach steady-state. It is under equilibrium conditions that the kinetic data should be collected, so as to ensure that the changes in the mercury concentration are solely due to the oxidation reaction, and not due to the sorption of Hg on the catalyst's surface.[34] In the current study, stationary conditions of mercury concentrations at the exit of the reactor were achieved after 3 to 6 h. At this point, the concentrations of Hg downstream of the catalyst were recorded only if the fluctuations of mercury concentration were smaller than 5 % for more than 30 min.[28,35]

Although the detection limit of the Hg analyzer used in this work is 2 ng/m^3, the precision of the analyzer was estimated based upon its reproducibility in detecting the Hg concentration under identical experimental conditions. The mercury concentrations are obtained by calibrating the analyzer prior to each experiment for known Hg flows. The experimental data is fitted to the calibration curves to obtain values of elemental and total mercury concentrations (C_{Hg^0} and $C_{Hg^{tot}}$). The uncertainties in the estimated parameters are obtained through the method of error propagation, which is explained by Taylor[36] and summarized in the Supporting Information.

The Hg raw data measured with the analyzer are transformed into mercury concentrations using the calibration equation. The concentration of Hg and its uncertainty are obtained as follows:

$$C_{Hg} = m_i x + b_i \rightarrow \sigma_{C_{Hg}} = \sqrt{x^2 \sigma_{m_i}^2 + \sigma_{b_i}^2} \quad (9)$$

where m_i and b_i are the slope and the intercept of the calibration line, respectively, and x is the Hg signal (raw data) from the analyzer. The error in the estimated Hg concentration, $\sigma_{C_{Hg}}$, depends on the variance of the slope ($\sigma_{m_i} = 0.0003$) and intercept ($\sigma_{b_i} = 0.4$) of the calibration line, which were estimated from calibrations carried out at identical conditions from different experiments. Note that the error associated with each concentration value is different since it depends on the value of the Hg signal, x.

Accordingly, the Hg oxidation efficiency and its uncertainty are giving by

$$X_{Hg} = \frac{C_{Hg^0}^{in} - C_{Hg^0}^{out}}{C_{Hg^0}^{in}} \rightarrow \sigma_X = \sqrt{\left(\frac{C_{Hg^0}^{out} \cdot \sigma_{C_{Hg^0}^{in}}}{(C_{Hg^0}^{in})^2} \right)^2 + \left(\frac{\sigma_{C_{Hg^0}^{out}}}{C_{Hg^0}^{in}} \right)^2} \quad (10)$$

where the first term inside the square root of eq 10 can be neglected since it is much smaller than the second term ($C_{Hg^0}^{out} < C_{Hg^0}^{in}$). Therefore, the error associated with the oxidation efficiency simplifies to

$$\sigma_X = \frac{\sigma_{C_{Hg^0}^{out}}}{C_{Hg^0}^{in}} \quad (11)$$

Using this expression for the uncertainty in the mercury oxidation, the oxidation rate and its uncertainty can be derived as

$$r_{Hg} = F_{Hg}^{in} \frac{X}{W} \rightarrow \sigma_{r_{Hg}} = \frac{F_{Hg}^{in}}{W} \sigma_X \quad (12)$$

The reaction orders, the effective reaction rate constants (k_{eff}) and the activation energy (E_A) are the slopes obtained after fitting the

experimental data to eqs 4, 7, and 8, respectively. The slopes of these functions and their error are calculated through weighted linear regression, which for brevity purposes, is explained in the Supporting Information. The uncertainties in the reaction orders (of O_2 and Hg), in the effective reaction rate constants and in the activation energy are shown as error bars in Figures 3, 4, and 5.

The magnitude of the errors in the Hg concentrations, oxidation efficiencies, and oxidation rates are summarized in Table S1 in the Supporting Information. The first two sets of experiments (effect of C_{O_2} and C_{Hg} on the oxidation rates) were carried out with 5 ppb of Hg in the inlet flue gas, which is too small given the level of uncertainty in measuring Hg concentrations at the exit of the reactor ($\sigma_{C_{Hg0}^{out}}$ varies from 0.17 to 1.14 ppb). To increase the concentration-to-error ratio, the rest of the experiments were performed with 15 ppb of inlet Hg concentration. The use of larger inlet mercury concentrations to minimize the relative error due to the continuous data acquisition is not unusual; the work done by Chen et al.,[32] an inlet mercury concentration of 20 ppb is used for this purpose.

Furthermore, the calibration curves obtained in these first sets of experiments, which are scattered in time, differ significantly. To account for this source of uncertainty, the variance in the slope and intercept of the calibration curves are included in eq 9 to determine the error in the Hg concentration. As a mean of comparison, Presto et al.[37] perform an error analysis on the oxidation of Hg, though considering novel catalysts instead of SCR catalysts. They report an average error of 10−20 % in the measured mercury concentration, which propagates to an error of 15−30 % in the estimated reaction rates.

RESULTS AND DISCUSSION

Reaction Order for O_2 and Hg. The reaction orders of O_2 and Hg on the oxidation rate need to be determined to develop an expression of the Hg oxidation rate. Both set of experiments were carried out for 0.05 g of catalyst and a total flow rate of 1300 mL/min (SV = 1 560 000 h^{-1}). These experiments were repeated for three temperatures to validate the reaction orders obtained. To test the influence of each gas, its concentration was varied while all of the other gas concentrations were kept constant.

The effect of the O_2 and Hg concentrations on the oxidation rates is shown in Figure 2, where the concentration of both gas components are expressed as increments for an easier comparison between the two. For the case of O_2, the concentrations tested (5, 7.5, and 10 %) are normalized by the 7.5 % concentration, while in the case of Hg, the concentrations tested (5.10, 6.37, 10.19, and 15.29 ppb) are normalized by the 10.19 ppb concentration. Dashed and solid lines help visualizing the trends of the oxidation rates as a function of the C_{O_2} and C_{Hg}, respectively. The first trend is that the increase in C_{Hg} leads to a linear increase in the oxidation rate (gray filled symbols). The second trend is the lack of variation in the mercury oxidation rate with increasing C_{O_2}, from its typical value in postcombustion conditions (5 %) to higher values (15 %). This result suggests that O_2 is not a limiting factor for mercury oxidation across the SCR catalyst since O_2 is always present in flue gas.

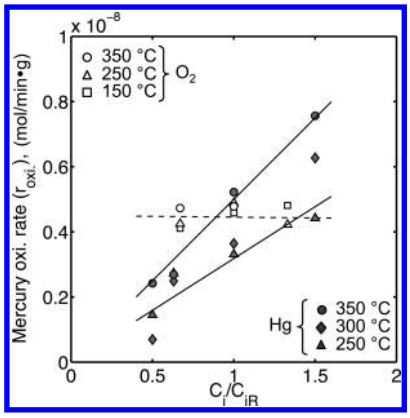

Figure 2. Rate of mercury oxidation as a function of normalized concentrations of O_2 and Hg. Dashed and solid lines help visualizing the trends of the oxidation rates as a function of the C_{O_2} and C_{Hg}, respectively.

To estimate the reaction order of O_2, the reaction rate values obtained at different O_2 concentration are fitted to eq 4 whose slope, b, is the reaction order as shown in eq 13.

$$-\ln(r_{Hg}) = \ln(k_{Hg}^{*}) + b\cdot\ln(C_{O_2}) \tag{13}$$

By plotting $-\ln(r_{Hg})$ vs $\ln(C_{O_2})$ and using the weighted linear regression method, the slopes and their errors can be obtained, as shown in Figure 3 (Left). The large error seen at 350 °C resulted from the large difference between the calibration curve of that experiment and the calibration curves obtained at 250 and 150 °C. As mentioned before, the variance in the slope and intercept of the calibration curves are included in the estimation of the error in the Hg concentration (larger spread on these values leads to larger errors in the concentration of Hg). The approximately zero slopes suggest a zeroth-order with respect O_2, which is in agreement with previous experimental studies.[28,38] This results justify our decision to not include O_2 in the expression of the oxidation rate used to determine the activation energy in the next section.

A similar procedure was used to study the reaction order of Hg in the mercury oxidation across the SCR catalyst. The oxidation rates obtained after varying the concentrations of Hg between 5 and 15 ppb at different temperatures were fitted to eq 4. The right side of Figure 3 shows the linear fits of $-\ln(r_{Hg})$ vs $\ln(C_{Hg})$ and the slopes, which are the reaction order of Hg. The scale of the y-axis was kept the same as in Figure 3a for an easier comparison between the two different gas components. The trend in the slopes suggest that Hg is first-order in the oxidation rate, which is in agreement with the work of Gao et al.[28]

It is important to notice that the reaction orders of O_2 and Hg are obtained under simplified flue gas conditions since NH_3 and NO are not included, however, even under these simplified conditions the uncertainty in the obtained kinetic parameters is mostly controlled by the uncertainty in the measured Hg concentrations. One could argue that there is a systematic difference in the slopes for O_2 and Hg at the lowest temperature (150 and 250 °C, respectively) compared to the slopes obtained at higher temperatures. Although the slopes appear to be different, the uncertainty associated with their slope does not allow drawing any conclusion with respect to a systematic difference.

Apparent Activation Energy for the Hg Oxidation Reaction. Determining the apparent activation energy is an important step in the activity analysis of any catalyst. This kinetic parameter was estimated by carrying out experiments where temperature and the amount of catalyst (W) were varied, while other operating conditions such as total flow rate (Q) and flue gas concentrations were kept constant. A summary of the oxidation efficiencies for three different amounts of catalyst (or

dx.doi.org/10.1021/ef502096r | Energy Fuels 2015, 29, 369−376

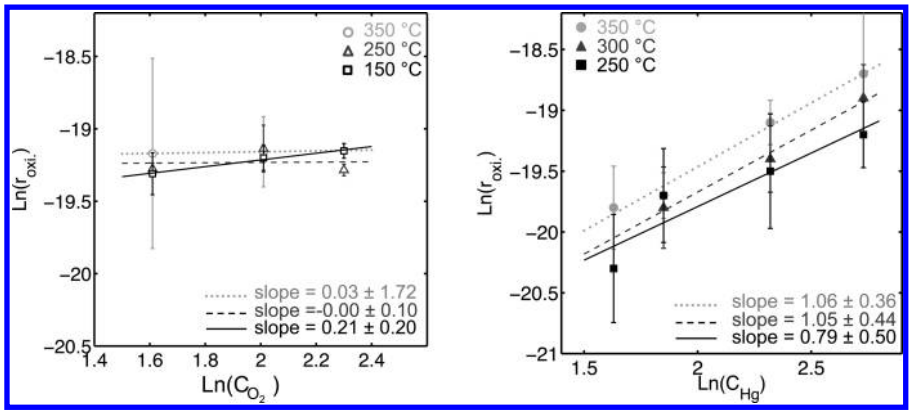

Figure 3. Left: Reaction order (slopes) for O_2 obtained from experiments with C_{O_2} of 5, 7.5, and 10 % of O_2 carried out at 150, 250, and 350 °C. Right: Reaction order for Hg (slopes) from experiments with C_{Hg} of 5.10, 6.37, 10.19, and 15.29 ppb carried out at 250, 300, and 350 °C.

equivalent space velocities) as a function of temperature are shown in Table 2.

As expected, the oxidation efficiency increases with the amount of catalyst (decreasing space velocity) due to the larger residence time of the flue gas in contact with the active catalyst sites. The dependence of the Hg oxidation with temperature is not trivial due to a more complex relationship with the operating conditions, namely, flue gas composition and temperature itself. The dependence on the flue gas composition can be appreciated by comparing results by Hocquel[39] and Richardson et al.[40] The laboratory work carried out by Hocquel using a simulated flue gas (Hg^0, HCl, O_2, H_2O, and N_2) on pure vanadium oxide powders shows an increase of the Hg oxidation for temperatures between 170 and 410 °C. On the other hand, the study performed by Richardson et al.[40] using a simulated flue gas that includes NH_3 shows that Hg oxidation decreases with increasing temperature after reaching a maximum at 315 °C. Interestingly enough, in the absence of NH_3 the maximum shifts to 370 °C. A qualitatively similar behavior is reported by Senior[41] with a maximum in the Hg oxidation observed at 350 °C. Therefore, the increase in the Hg oxidation with temperature observed in the present study is in agreement with these previous findings, since the simulated flue gas does not contain NH_3 and the operating temperatures are in the low regime (350 °C and below). Furthermore, the experiment carried out at the lowest temperature (200 °C) shows a linear dependence of the oxidation efficiency with the amount of catalyst, thereby justifying the assumption in eq 3 ($r_{Hg} = F^{in}_{Hg}(dX/dW) \approx F^{in}_{Hg}(X/W)$).

The equation used to determine the activation energy corresponds to the differential reactor and it is only valid for low conversion regimes. To work within the validity limits of this equation, only the reaction rates corresponding to low mercury efficiency (lower than 50 %) in Table 2 were used to determine the activation energy, E_A. Using eq 7, the effective rate constant (k_{eff}) at different temperatures was determined from the slopes of the plots $-\ln(1 - X)$ vs W/Q as shown in Figure 4, where for each temperature, filled and empty symbols correspond to reaction rates with mercury efficiencies lower and higher than 50 %, respectively.

The effective reaction rate constants obtained from the slopes of the linear fits in Figure 4 do not include most of the experimental points since they correspond to large oxidation efficiencies. Although using the linear fits with only two data points may be limiting, it was shown that for efficiencies below

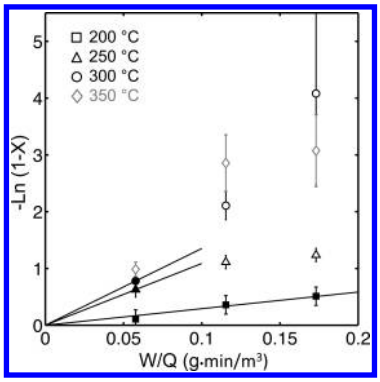

Figure 4. Graphical estimation of the k_{eff} as a function of T.

50 %, the oxidation efficiency and the amount of catalyst were linearly dependent (data points at 200 °C). We believe that the same linear behavior should be expected at higher temperatures within a low efficiency range, thereby justifying our approach.

A possible way to ensure lower oxidation efficiencies is to increase the space velocity (decreasing the amount of catalyst and keeping constant the total flow rate) since the residence time would decrease; however, this solution could not be implemented in the current set-up. An attempt to work with a lower amount of catalyst (<0.05 g) led to a channeling problem (instantaneous breakthrough), where large portions of the flow rate pass through the catalyst bed without contacting the catalyst. As a result, inaccurate readings of mercury concentrations at the exit of the packed-bed reactor were obtained, suggesting 0.05 g as the minimum amount of catalyst required in our set-up.

The error bars in Figure 4 increase at high temperature when higher oxidation efficiencies were obtained. The dependence of this error on the X is shown in the eq 19 of the Supporting Information. However, since only values corresponding to oxidation efficiencies below 50 % are linearly fitted in Figure 4, the error associated with those slopes remains relatively small. The effective reaction rate constants, k_{eff}, obtained from the slopes are fitted to eq 8 to obtain graphically the effective activation energy, E_A, as shown in Figure 5.

Under the simplified flue gas condition tested (i.e., NH_3 and NO are not included), the apparent activation energy, E_A, obtained is 34 ± 7 kJ/mol (± 14 kJ/mol for a 95 % confidence interval). This value is in reasonable agreement with the activation energy of 37.73 kJ/mol reported by Gao et al., who

dx.doi.org/10.1021/ef502096r | Energy Fuels 2015, 29, 369−376

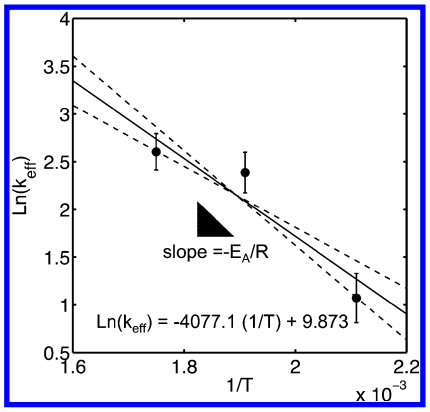

Figure 5. Graphical estimation of the E_A from the effective reaction constants, k_{eff}, obtained at different temperatures in Figure 4. The dashed lines represent fits that consider one standard deviation in both slope and intercept (68 % confidence interval).

studied the effect of HCl on Hg oxidation in air across a standard SCR catalyst.[28] It is worth mentioning several differences between the current study and the work done by Gao et al. In our study, a more complex simulated flue gas is used, which includes the presence of CO_2 and water vapor, which affects the activity of the SCR catalyst. For example, water vapor that inevitably exists in the flue gas has a significant effect on the catalytic activity, such as competition for adsorption sites[23,35] or the strong interaction with the support of the SCR catalyst.[26,42] More importantly, the reaction rates used by Gao et al. to determine the activation energy correspond to high Hg oxidation efficiencies, where the differential reactor equation does not hold (only 2 out of 12 reaction rates used in their kinetic analysis correspond to efficiencies below 50 %). The use of high conversion efficiency values may lead to an inaccurate activation energy value. To illustrate the sensitivity of the activation energy with the oxidation rates and oxidation efficiencies, an alternative activation energy was calculated using all of the oxidation rates obtained in this study (linearly fitting all the points in Figure 4). In this case, an activation energy of 45 ± 8 kJ/mol was obtained, which is significantly larger than the value obtained by using only the low-conversion data.

CONCLUSIONS

The effect of flue gas composition, temperature, and space velocity on the Hg oxidation efficiency of a standard composition SCR catalyst is revisited, confirming that O_2 is zeroth-order, while Hg is first-order in terms of the Hg oxidation rate. An activation energy of 34 ± 7 kJ/mol is obtained. The magnitude of the oxidation efficiencies increases with increasing amount of catalyst and temperature (from 150 to 350 °C). Even under the simplified flue gas conditions tested (i.e., NH_3 and NO are not included), the uncertainty in the reaction rates and kinetic parameters is mostly controlled by the uncertainty in the measured Hg concentrations.

The results of this study reveal several important aspects of the Hg oxidation lab-scale experiments and their current limitations. An essential step in any experimental analysis is the quantification of the error associated with the measured parameter, which can be reduced by modifying the experimental procedure. We observed that the significant variability of the calibration curve affects the precision of the measured Hg concentration, even when identical experimental conditions were set. This source of uncertainty was included in the error analysis, and, accordingly, errors in the oxidation rates, reaction orders and activation energies were quantified. We propose that working with larger molar flows of Hg leads to the reduction of the uncertainty in the Hg concentrations and in the properties thereby derived. Furthermore, we emphasize the importance of working within the low-conversion efficiency regime, where the differential reactor equation holds. However, the modification the operating conditions to reach such low efficiencies can be limited by size of the equipment or the operating times.

ASSOCIATED CONTENT

Supporting Information

Apparatus; kinetic analysis of packed-bed reactors; kinetic analysis, mechanism and rate-limiting steps; assessment of the Hg measurements precision. This material is available free of charge via the Internet at http://pubs.acs.org.

AUTHOR INFORMATION

Corresponding Author

*E-mail: anasn@alumni.stanford.edu.

Notes

The authors declare no competing financial interest.

ACKNOWLEDGMENTS

The Stanford University School of Earth Sciences Graduate Fellowship Program supported this work. The authors thank Dr. Dave Thompsett, Dr. Michael Nash, and Silvia Alcove at Jonhson Matthey Technology Center (Reading, U.K.) for their technical feedback.

REFERENCES

(1) Rafaj, P.; Bertok, I.; Cofala, J.; Schöpp, W. Scenarios of global mercury emissions from anthropogenic sources. *Atmos. Environ.* **2013**, *79*, 472−479.

(2) Krabbenhoft, D. P.; Sunderland, E. M. Global change and mercury. *Science* **2013**, *341*, 1457−1458.

(3) *Environmental Footprints and Cost of Coal-Based Integrated Gasification Combined Cycle and Pulverized Coal Technologies*; Report from the United States Environmental Protection Agency; EPA: Washington, DC, July, 2006.

(4) Karagas, M. R.; Choi, A. L.; Oken, E.; Horvat, M.; Schoeny, R.; Kamai, E.; Cowell, W.; Grandjean, P.; Korrick, S.; et al. Evidence on the human health effects of low-level methylmercury exposure. *Environ. Health Perspect.* **2012**, *120*, 799.

(5) *Mercury and Air Toxics Standards (MATS) for Power Plants, Federal Register*; Report from the United States Environmental Protection Agency; EPA: Washington, DC, Feb. 16, 2012; Vol. 77, p 9302.

(6) Pavlish, J. H.; Sondreal, E. A.; Mann, M. D.; Olson, E. S.; Galbreath, K. C.; Laudal, D. L.; Benson, S. A. Status review of mercury control options for coal-fired power plants. *Fuel Process. Technol.* **2003**, *82*, 89−165.

(7) Niksa, S.; Fujiwara, N. A predictive mechanism for mercury oxidation on selective catalytic reduction catalysts under coal-derived flue gas. *J. Air Waste Manage. Assoc.* **2005**, *55*, 1866−1875.

(8) Brown, T.; Smith, D.; Hargis, R., Jr; O'Dowd, W. Mercury measurement and its control: What we know, have learned, and need to further investigate. *J. Air Waste Manage. Assoc.* **1999**, *49*, 628−640.

(9) Senior, C.; Linjewile, T. *Oxidation of Mercury Across SCR Catalyst in Coal-Fired Power Plants Burning Low Rank Fuels*; Technical Report; Reaction Engineering International: Salt Lake City, UT, 2003.

(10) Niksa, S.; Helble, J. J.; Fujiwara, N. Kinetic modeling of homogeneous mercury oxidation: The importance of NO and H_2O in

predicting oxidation in coal-derived systems. *Environ. Sci. Technol.* **2001**, *35*, 3701−3706.
(11) Cauch, B.; Silcox, G. D.; Lighty, J. S.; Wendt, J. O.; Fry, A.; Senior, C. L. Confounding effects of aqueous-phase impinger chemistry on apparent oxidation of mercury in flue gases. *Environ. Sci. Technol.* **2008**, *42*, 2594−2599.
(12) Padak, B.; Wilcox, J. Understanding mercury binding on activated carbon. *Carbon* **2009**, *47*, 2855−2864.
(13) Presto, A.; Granite, E. Survey of catalysts for oxidation of mercury in flue gas. *Environ. Sci. Technol.* **2006**, *40*, 5601−5609.
(14) *EPRI Technical Report No. 1005400*; Electric Power Research Institute: Palo Alto, CA, 2002.
(15) Staudt, J. E. *Control Technologies to Reduce Conventional and Hazardous Air Pollutants from Coal-Fired Power Plants*; Technical Report; Andover Technology Inc.: Andover, MA, 2011.
(16) Eom, Y.; Jeon, S.; Ngo, T.; Kim, J.; Lee, T. Heterogeneous mercury reaction on a selective catalytic reduction (SCR) catalyst. *Catal. Lett.* **2008**, *121*, 219−225.
(17) He, S.; Zhou, J.; Zhu, Y.; Luo, Z.; Ni, M.; Cen, K. Mercury oxidation over a vanadia-based selective catalytic reduction catalyst. *Energy Fuels* **2008**, *23*, 253−259.
(18) Gale, T. K.; Merritt, R. L.; Cushing, K. M.; Offen, G. R. Mercury speciation as a function of flue gas chlorine content and composition in a 1 MW semi-industrial scale coal-fired facility. *Proceedings of the Mega Symposium and Air & Waste Management Association's Specialty Conference, Washington, DC,* 2003.
(19) Pavlish, J. H.; Holmes, M. J.; Benson, S. A.; Crocker, C. R.; Galbreath, K. C. Application of sorbents for mercury control for utilities burning lignite coal. *Fuel Process. Technol.* **2004**, *85*, 563−576.
(20) Cao, Y.; Gao, Z.; Zhu, J.; Wang, Q.; Huang, Y.; Chiu, C.; Parker, B.; Chu, P.; Pan, W.-p. Impacts of halogen additions on mercury oxidation, in a slipstream selective catalyst reduction (SCR), reactor when burning sub-bituminous coal. *Environ. Sci. Technol.* **2007**, *42*, 256−261.
(21) YANG, H.-m.; PAN, W.-P. Transformation of mercury speciation through the SCR system in power plants. *J. Environ. Sci.* **2007**, *19*, 181−184.
(22) Lee, C. W.; Srivastava, R. K.; Ghorishi, S. B.; Karwowski, J.; Hastings, T. W.; Hirschi, J. C. Pilot-scale study of the effect of selective catalytic reduction catalyst on mercury speciation in Illinois and Powder River Basin coal combustion flue gases. *J. Air Waste Manage. Assoc.* **2006**, *56*, 643−649.
(23) Li, H.; Li, Y.; Wu, C.-Y.; Zhang, J. Oxidation and capture of elemental mercury over SiO_2−TiO_2−V_2O_5 catalysts in simulated low-rank coal combustion flue gas. *Chem. Eng. J.* **2011**, *169*, 186−193.
(24) Stolle, R.; Koeser, H.; Gutberlet, H. Oxidation and reduction of mercury by SCR DeNOx catalysts under flue gas conditions in coal fired power plants. *Appl. Catal. B: Environ.* **2014**, *144*, 486−497.
(25) Lee, C. W.; Srivastava, R. K.; Ghorishi, S. B.; Hastings, T. W.; Stevens, F. M. Investigation of selective catalytic reduction impact on mercury speciation under simulated NOx emission control conditions. *J. Air Waste Manage. Assoc.* **2004**, *54*, 1560−1566.
(26) Suarez Negreira, A.; Wilcox, J. DFT study of Hg oxidation across vanadia−titania SCR catalyst under flue gas conditions. *J. Phys. Chem. C* **2013**, *117*, 1761−1772.
(27) Suarez Negreira, A.; Wilcox, J. Role of WO_3 in the Hg oxidation across the V_2O_5−WO_3−TiO_2 SCR catalyst: A DFT study. *J. Phys. Chem. C* **2013**, *117*, 24397−24406.
(28) Gao, W.; Liu, Q.; Wu, C.-Y.; Li, H.; Li, Y.; Yang, J.; Wu, G. Kinetics of mercury oxidation in the presence of hydrochloric acid and oxygen over a commercial SCR catalyst. *Chem. Eng. J.* **2013**, *220*, 53−60.
(29) Rallo, M.; Heidel, B.; Brechtel, K.; Maroto-Valer, M. M. Effect of SCR operation variables on mercury speciation. *Chem. Eng. J.* **2012**, *198*, 87−94.
(30) Niksa, S.; Freeman Sibley, A. Predicting the multipollutant performance of utility SCR systems. *Ind. Eng. Chem. Res.* **2010**, *49*, 6332−6341.
(31) Madsen, K.; Jensen, D.; Frandsen, J.; Thogersen, R. A mechanistic Study on the Inhibition of the DeNOx Reaction on the Mercury Oxidation over SCR catalysts. *Proceedings of Air Quality VIII Conference*; 2011.
(32) Chen, W.; Ma, Y.; Yan, N.; Qu, Z.; Yang, S.; Xie, J.; Guo, Y.; Hu, L.; Jia, J. The co-benefit of elemental mercury oxidation and slip ammonia abatement with SCR-Plus catalysts. *Fuel* **2014**, *133*, 263−269.
(33) Fogler, H. S. *Elements of Chemical Reaction Engineering*; Prentice-Hall International: London/New Jersey, 1999.
(34) Presto, A. A.; Granite, E. J.; Karash, A.; Hargis, R. A.; O'Dow, W. J.; Pennline, H. W. A kinetic approach to the catalytic oxidation of mercury in flue gas. *Energy Fuels* **2006**, *20*, 1941−1945.
(35) Zhang, M.; Wang, P.; Dong, Y.; Sui, H.; Xiao, D. Study of elemental mercury oxidation over an SCR catalyst with calcium chloride addition. *Chem. Eng. J.* **2014**, *253*, 243−250.
(36) Taylor, J. R. *An Introduction Error Analysis: The Study of Uncertainties in Physical Measurements*; University Science Books: Herndon, VA, 1997.
(37) Presto, A.; Granite, E. Noble metal catalysts for mercury oxidation in utility flue gas. *Platinum Met. Rev.* **2008**, *52*, 144−154.
(38) Li, Y.; Murphy, P. D.; Wu, C.-Y.; Powers, K. W.; Bonzongo, J.-C. J. Development of silica/vanadia/titania catalysts for removal of elemental mercury from coal-combustion flue gas. *Environ. Sci. Technol.* **2008**, *42*, 5304−5309.
(39) Hocquel, M. Ph.D. thesis, University of Stuttgart, Germany, 2003.
(40) Richardson, C.; Machalek, T.; Miller, S.; Dene, C.; Chang, R. Effect of NOx control processes on mercury speciation in utility flue gas. *J. Air Waste Manage. Assoc.* **2002**, *52*, 941−947.
(41) Senior, C. L. Oxidation of mercury across selective catalytic reduction catalysts in coal−fired power plants. *J. Air Waste Manage. Assoc.* **2006**, *56*, 23−31.
(42) Vittadini, A.; Selloni, A.; Rotzinger, F.; Grätzel, M. Structure and energetics of water adsorbed at TiO_2 anatase 101 and 001 surfaces. *Phys. Rev. Lett.* **1998**, *81*, 2954−2957.